East European Journal of Physics. 4. 159-166 (2023)
DOI:10.26565/2312-4334-2023-4-17 ISSN 2312-4334

LATERAL PHOTOELECTRIC EFFECT IN IRON-SILICON DIOXIDE-COMPENSATED SILICON HYBRID STRUCTURES

Eshkuvat U. Arzikulov[a,*], Alisher D. Nurimov[a], F.A. Salakhitdinov[a], U.A. Ashirov[a], T.S. Sharafova[a], A.Sh. Khujanov[b], R.M. Usanov[a]

[a] *Samarkand State University named after Sharof Rashidov, 140000, Samarkand, University Blvd. 15, Republic of Uzbekistan; e-mail: rectorl@samdu.uz*

[b] *Samarkand State University of Veterinary Medicine, Livestock and Biotechnologies, 140003, Samarkand, Mirzo Ulug'bek str. 77, Republic of Uzbekistan*

**Corresponding Author e-mail: eshkuvata@gmail.com; Tel.: (+998915389791)*

Received August 6, 2023; revised September 21, 2023; accepted September 21, 2023

This article presents experimental results on the technology of obtaining and studying the lateral photoelectric effect (LPE) in hybrid structures (HS) of the Fe/SiO_2/p-Si<B, Mn> and Fe/SiO_2/n-Si<B, Mn> types. The technology for obtaining such HS consists of two parts: firstly, obtaining compensated (C), highly compensated (HC), and over-compensated (OC) samples of Si <B, Mn>. Secondly, obtaining HS Fe/SiO_2/p-Si<B, Mn> and Fe/SiO_2/n-Si<B, Mn>. Based on the results, it is shown that sufficiently good HS has been obtained. Experiments on the study of LPE have shown that in the studied HS there is a pronounced manifestation of the lateral photoelectric effect, the magnitude and nature of which strongly depend on the type of conductivity and resistivity of the compensated silicon. The observed features are explained by the fact that in C, HC, and OC silicon samples, impurities that create deep levels in the silicon band gap form various multi-charged complexes that modulate the energy band of silicon, which lead to significant changes in its physicochemical and generation-recombination properties, which underlies the observed effects. Based on the LPE studies, depending on the contact distance, it is possible to determine the numerical values of the diffusion lengths of the minor current carriers (L_p and L_n), their lifetimes (τ_p and τ_n), and diffusion coefficients (D_p and D_n) on the substrate material.

Keywords: *Lateral photo effect; Hybrid structure; Compensated silicon; Photovoltage; Diffusion; Evaporation; Oxide; p-n junction*

PACS: 68.37.Ps; 68.65.Ac; 78.20.−e; 73.30.+y; 73.43.Qt; 81.10.Bk; 81.65.Cf

INTRODUCTION

Although the discovery of LPE was first reported in 1930 by the German physicist Schottky [1], his pioneer in world literature is considered to be Wallmark, who published an article on this topic in 1957 [2]. Since then, LPE in semiconductor structures has been intensively studied due to its wide practical application in optoelectronic devices, especially as position-sensitive sensors, since the LPE arising in them varies linearly with the distance relative to the contacts. LPE occurs with uniform illumination of the p-n junction as a result of lateral diffusion and recombination of photogenerated electron-hole pairs [3-4]. A similar effect has also been studied in metal-semiconductor (MS) structures [5-10] and metal-oxide-semiconductor (MOS) [11-17]. In the last decade, so-called silicon-based hybrid structures, which are essentially MOS structures, have been intensively studied [19-23].

Analysis of existing works has shown that in the studied structures, low-resistance plates of monocrystalline silicon were mainly used as a semiconductor substrate with n- and p-types of conductivity: p-Si $\rho = 4.5 \div 8.3$ Ω×cm and n-Si $\rho = 7.5 \div 80$ Ω ×cm, respectively [11, 12, 18, 22, 24-25]. Despite the existence of a number of studies devoted to the influence of the type of conductivity of substrates on their photovoltaic properties, there is currently no justification for the choice of substrate material.

In this connection, there is an interest in the use of C, HC and OC samples of monocrystalline silicon doped with various impurities as substrates in such structures by high-temperature diffusion. It is known that C, HC, and OC silicon samples have unique physical properties, namely, high photosensitivity in both the impurity and intrinsic spectral regions [26], infra-low-frequency oscillations of the photocurrent with a large amplitude [27-28], recombination waves [29-30], large positive and negative magnetoresistance [31-32], deep temperature and infrared quenching of photoconductivity [33-34], etc. In addition, the reproducible technology for producing compensated silicon with various impurities has reached its perfection and can be used as an additional degree of freedom both in controlling the parameters of the HS technology and in controlling the effects observed in them.

RESULTS AND DISCUSSION

Technology for obtaining C, HC, and OC silicon samples

The production of HS consists of two stages. In the first stage, it is necessary to obtain C, HC, and OC silicon samples doped with manganese atoms by the high-temperature diffusion method. To do this, samples of $8\times5\times0.5$ mm^3 in the form of a parallelepiped with a crystallographic orientation [100] were cut from the original silicon plates of the

Cite as: E.U. Arzikulov, A.D. Nurimov, F.A. Salakhitdinov, U.A. Ashirov, T.S. Sharafova, A.Sh. Khujanov, R.M. Usanov, East Eur. J. Phys. 4, 159 (2023), https://doi.org/10.26565/2312-4334-2023-4-17

KDB-10 brand (boron-doped silicon with a specific electrical resistance of 10 Ω×cm at room temperature) used in the electronics industry. To remove the damaged surface layer formed during plate cutting, the samples were first subjected to mechanical and then chemical treatment with HF: HNO_3 etchant. The state of the surface of the initial substrate p-Si<B> after chemical cleaning was studied using AFM in static force mode (Fig. 1).

The surface texture of the p-Si<B> substrate was measured in an area with horizontal dimensions of 60 μm×60 μm and vertical dimensions of 20 nm. Figure 1 on the left shows the image of the data obtained on the Z axis, and the image of the data obtained in the XY plane is placed on the right. The surface roughness parameters are given in Table 1.

Based on the results obtained, it can be said that the roughness parameters of the chemically treated surface show that such a surface is smooth enough to obtain HS. There are almost no hills or deep valleys on the surface. The results show that the chemical cleaning of the substrate p-Si<B> provides a smooth surface texture.

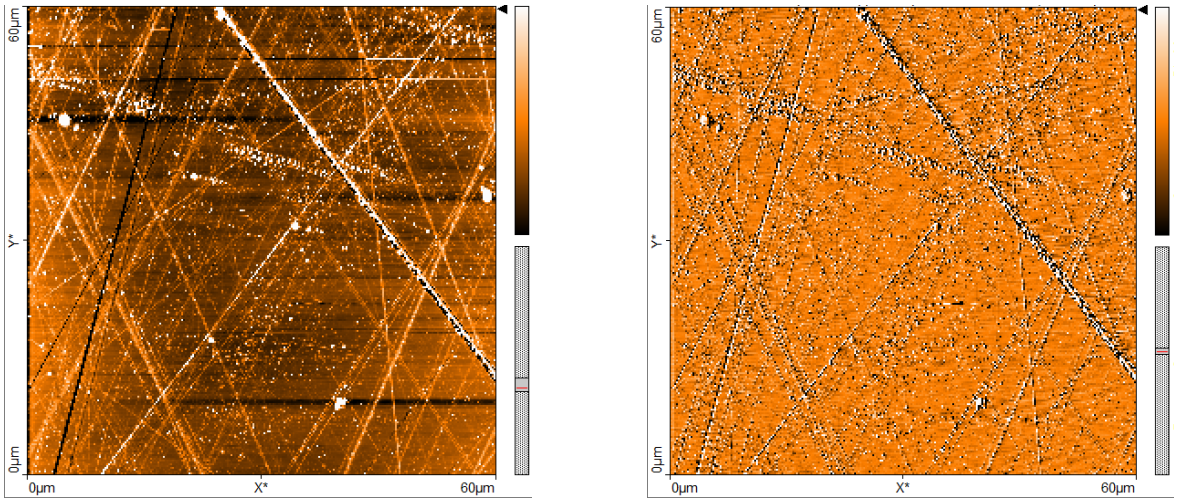

a) b)

Figure 1. 2D AFM image of the surface of the initial samples p-Si<B> taken (60 μm×60 μm) along the Z axis and along the XY plane in static force mode

High-temperature diffusion alloying of manganese into silicon was carried out according to a well-known technique [35]. The initial silicon samples with manganese impurities were placed in a pre-purified quartz ampoule and air was pumped out of the ampoule to a pressure of ~ 10^{-5} mm Hg. The diffusion of manganese into silicon was carried out in a horizontal furnace of the SOUL-4.0 type, which ensures the maintenance of a constant temperature with an accuracy of ± 0.1°C for two hours. The temperature in the working area of the furnace was additionally controlled using a type B thermocouple (a combination of platinum alloys (6% rhodium) or platinum (30% rhodium).

Table 1. Roughness parameters of the p-Si<B> substrate and Fe layers.

Surface	R_m, fm	R_a nm	R_q nm	R_y nm	R_p nm	R_v nm
p-Si<B>	-41.355	1.528	3.327	145.71	104.73	-40.979
Fe	-19.009	26.446	33.783	254.31	167.74	-86.575

After the diffusion stage was completed, the samples were rapidly cooled at a rate of 120-150 °C/s to a temperature of 18°C. To obtain samples with different values of electrical resistivity and types of conductivity, the diffusion temperature was varied in the range of 1020÷1060 °C. After the process of high-temperature diffusion, a manganese-enriched layer with a thickness of about 15-20 microns is formed on the surface of the samples. To remove this layer, the obtained samples were also subjected to mechanical and chemical treatment, as well as the original samples. To determine the main parameters (electrical resistivity (ρ), concentration (n) and mobility of current carriers (μ)) the Hall effect method was used for both initial and doped samples [36]. This diffusion technology makes it possible to obtain C, HC and OC silicon samples doped with manganese with both p- and n-types of conductivity, with a resistivity in the range of $\rho \approx 10^2 \div 10^5$ Ω×cm at room temperature.

It is known that in C, HC and OC samples of silicon, the impurity atoms that create deep energy levels in its band gap in a charged state. The multiplicity of their charge depends on the degree of compensation. In addition, these charged atoms can combine into complex multicharged clusters, which, in turn, leads to noticeable changes in both the energy band of silicon and its generation-recombination parameters [26]. In the case of an impurity of manganese having a sufficiently large diffusion coefficient at high temperatures, its atoms can be in one- and two-times positively charged states, and can also be part of multicharged complexes of the type $[Mn^+]^4$ [31], which, in turn, determines the basic physical properties of C, HC and OC Silicon samples, as well as HS, which they are part of. Thus, it can be concluded that the main parameters of C, HC and OC of silicon samples doped with manganese, as well as HS based on it, are

determined by the deep energy levels of the manganese atom in the silicon band gap. In addition, by regulating the diffusion temperature, the vapor pressure of the diffusant and the cooling rate of the samples, it is possible to control the basic physical parameters of C, HC and OC of silicon samples and HS based on it within a wide range [26].

Technology for obtaining HS

At the second stage, it is necessary to obtain a HS of the Fe/SiO_2/p(n)-Si<B, Mn> type. It has been shown that the properties of MOS HS are mainly determined by the thickness of the metal and oxide layers that provide tunneling of carriers through them. At the same time, it was found that the optimal thickness of the oxide layer is up to 5 nm, and the metal layer is 15 nm [24]. The growth of an oxide layer with a thickness of about 5 nm on the surface of diffusion-doped samples of n(p)-Si<B, Mn> was carried out according to the method described in the ref. [21, 41]. Then, layers of pure iron were obtained on the surface of purified and dried C, HC and OC samples of p(n)-Si<B, Mn> by thermal or electron beam evaporation in high vacuum [37]. The surface characteristics of the HS deposited by a thin layer of Fe were re-investigated using AFM in the static force mode (Figure 2).

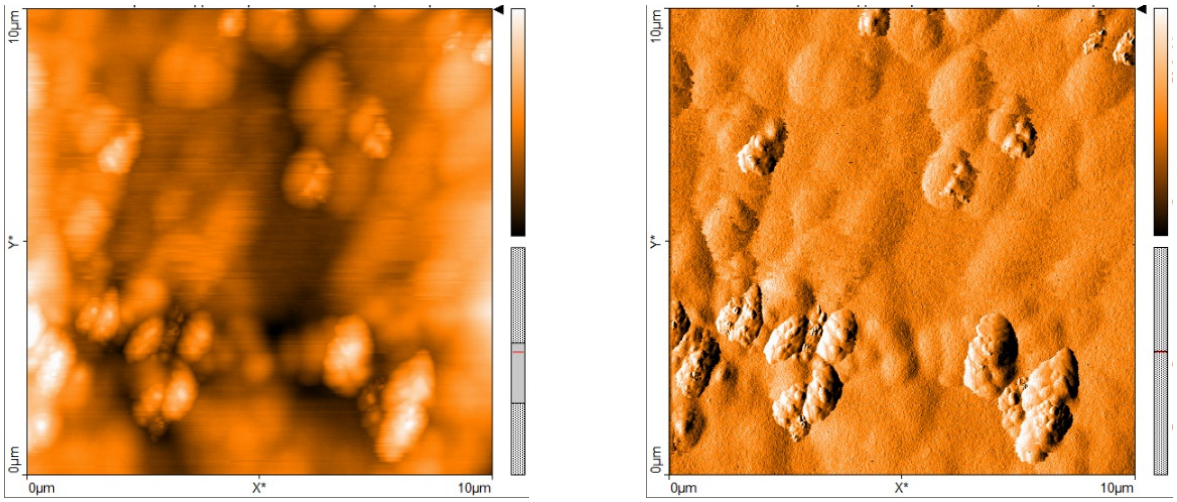

a) b)

Figure 2. Two-dimensional AFM images of the surface (10 µm×10 µm) of the iron layer in the Fe/p-Si hybrid structure in the Z axis (a) and in the XY plane (b) obtained in the "static force mode"

As in Figure 1, the left part of the figure shows an image of the Z axis, and the right part shows an image of data in the XY plane. The surface of the Fe film has the shape of hills and valleys. The average roughness of the substrate decreased from -41 fm to -19 fm as a thin layer of Fe was deposited. At the same time, the average roughness increased from 1.5 nm to 26.4 nm. A decrease in the average roughness value from -41 fm to -19 fm and an increase in the mean square (RMS) roughness value of the substrate from 1.5 nm to 26.4 nm during the formation of a thin layer of iron means that during the formation of a thin layer of iron on the silicon surface, Fe pairs covered the porosity of the surface caused by chemical cleaning, but the average roughness increased due to uneven distribution porosity on the surface. If you pay attention to the image of the surface, you can see several roughness of the granular form. Such a sharp change in the RMS of irregularities can be explained by the formation of these grains. The peak height value increased from 104.7 nm to 167.74 nm, and the depression depth value increased from -41 nm to -86.575 nm. This can be explained by the inhomogeneous distribution of evaporated Fe over the silicon surface. This, in turn, provides an increase in the height of the peaks of the valley. As the surface roughness increases, the probability of adsorption of charged particles on the crystal film increases, which can be explained by the fact that high temperatures can stimulate the migration of grain boundaries [38]. In addition, at high temperatures they can diffuse and occupy the right place in the crystal lattice, and grains with lower surface energy will increase at high temperatures [39]. In addition, the surface roughness of conductive thin films has a significant effect on the electrical characteristics of electronic devices manufactured on their basis [40].

The experiments conducted to study the I-V characteristics showed that good HS were obtained. Figure 4 shows the I-V dependence for one of the obtained HS at different values of the external magnetic field. As can be seen from Figure 4, I-V dependence shows good rectifying properties of HS and has a significant negative magnetoresistance. Thus, we can say that on the basis of the described technology, it is possible to obtain sufficiently good HS with a Schottky barrier of the Fe/SiO_2/p(n)-Si<B, Mn> type.

If we compare the images, then after the deposition of iron on a chemically treated silicon substrate, the grain size increased, which can be explained by the inhomogeneous distribution of iron atoms deposited on the surface during the evaporation of pure iron. However, the surface roughness can be analyzed based on the data obtained using AFM. Table 1 shows that initially the average roughness on the silicon substrate is about 1.5 nm, but after applying the iron layer, this value is 26.4 nm, which means that the surface roughness of the iron layer is significantly higher than the base. Comparing the values of the RMS, we can say that the roughness on the surface of the silicon base is due to the inhomogeneous

placement of Fe atoms on the silicon base, that is, the surface has a granular texture. In conclusion, we can say that the surface of the iron layer in the Fe/p-Si<B> HS has a high hardness and a granular surface. This kind of research provides a more complete understanding of the influence of shooting conditions and modes on the morphology of thin films and can help in adapting deposition parameters in accordance with the requirements of surface topography for electronic device applications.

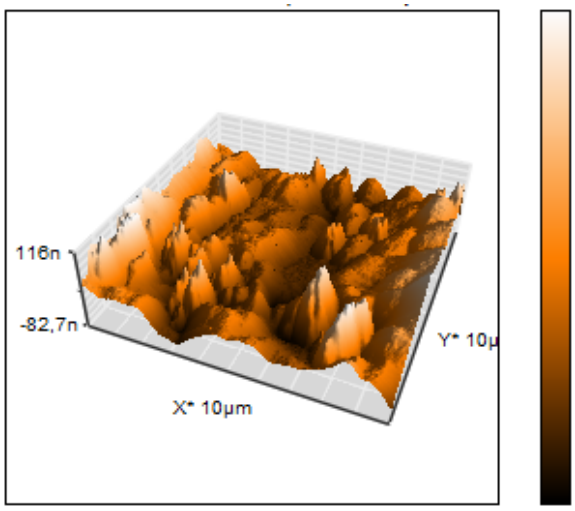

Figure 3. Three-dimensional images of the surface (10 μm×10 μm) of the iron layer in Fe/SiO_2/p-Si HS

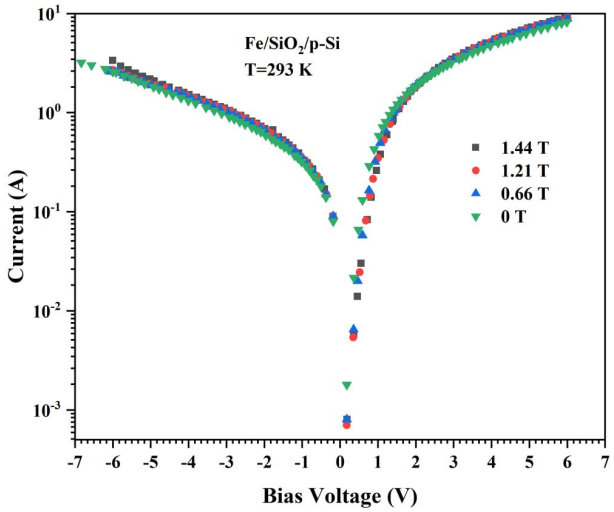

Figure 4. I-V dependence for one of the obtained HS Fe/SiO_2/p-Si under an external magnetic field

Lateral photoeffect in HS

The experimental setup described in [25] was used for the experimental study of LPE in the HS. Diode-pumped semiconductor lasers with wavelengths of 532 and 632 nm were used as a light source. Experiments conducted at T=293 K showed that pronounced LPE is observed in the studied HS and the value of lateral photovoltage (LPV) is higher than in the previously studied structures [2]. The sensitivity of the LPE is 1648.5 μV/mm. Figure 5 shows the dependence of the LPV on the distance between the contacts for HS based on the initial samples of p-Si<B>.

The electrical resistivity of the sample ρ = 10 Ω×cm, the wavelength and laser power λ = 632 nm and 8 mW, respectively, T = 293 K. As can be seen from Figure 5, the dependence of the LPV on the contact distance for the HS manufactured on the basis of the initial samples of p-Si <B> has a linear character, which corresponds to the results of theoretical [2, 3] and experimental studies [4]. We have studied the LPE in the HS Fe/SiO_2/p-Si<B, Mn> and Fe/SiO_2/n-Si<B, Mn> under the same conditions as in the HS manufactured on the basis of the initial samples of p-Si<B>. The results of the experiments are shown in Fig. 6. As can be seen from Figure 6, both Fe/SiO_2/p-Si<B, Mn> and Fe/SiO_2/n-Si<B, Mn> have LPE.

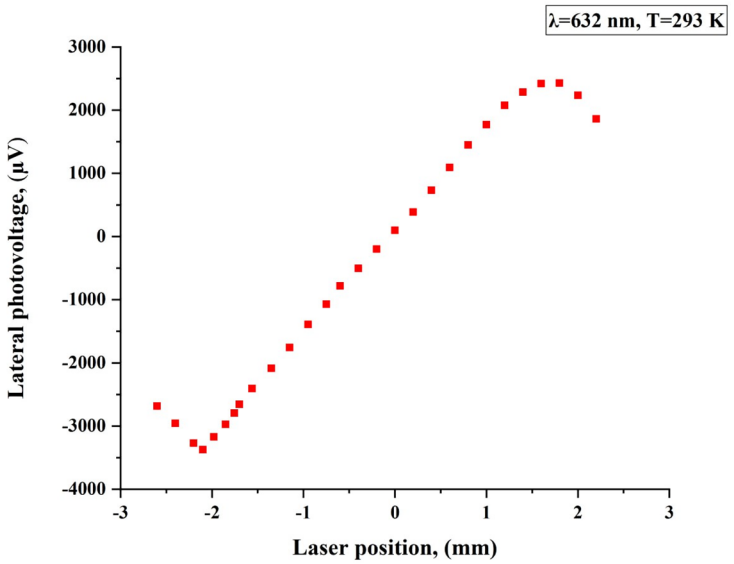

Figure 5. The dependence of the LPV on the distance between the contacts for the initial structure of p-Si<B>. Electrical resistivity of the sample ρ= 10 ohms × cm, λ = 632 nm, T = 293 K, laser power: 8 MW.

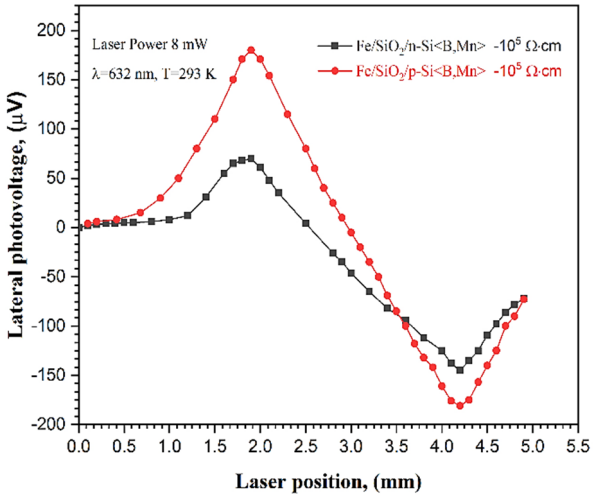

Figure 6. Dependence of the LPV on the distance between the contacts for the Fe/SiO_2/p-Si<B, Mn> and Fe/SiO_2/n-Si<B, Mn> HSs.

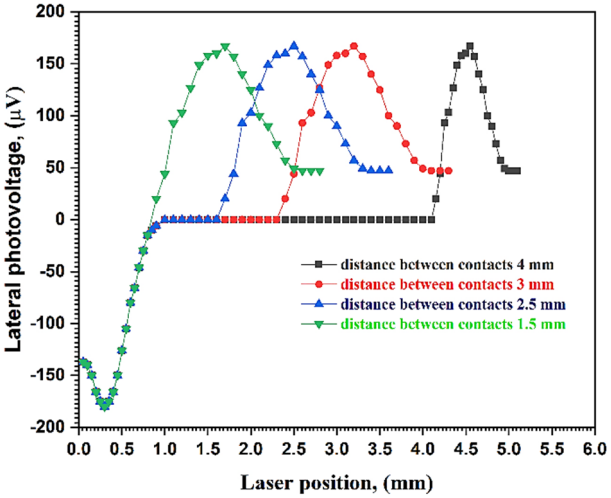

Figure 7. Dependence of the LPV on the distance between the contacts for the Fe/SiO_2/p-Si<B, Mn> HS. Sample electrical resistivity is $\rho = 1 \cdot 10^5$ Ω×cm, λ= 532 nm, T = 300 K, Laser power: 8 mW.

When the type of conductivity of C, HC and OC of silicon samples is changed, an inversion of the LPV polarity is observed, which is explained by the fact that in the Fe/SiO2/n-Si<B, Mn> structure, the internal field of the transition is directed from silicon to a thin layer of iron, and in Fe/SiO_2/p-Si<B, Mn> from the iron layer to silicon, which is due to the presence of interface states at the Fe/SiO_2/Si<B, Mn> boundary [18]. For both structures, there is an extreme dependence of the LPV on the thickness of the Fe film with a maximum localized near ~ 5 nm. It is assumed that in the Fe/SiO_2/Si<B, Mn> HSs, due to the high resistivity of C, HC and OC silicon samples, the characteristics of the LPE are determined by the processes of lateral diffusion of excess photogenerated carriers drawn by the built-in barrier field from the silicon volume into the area adjacent to the Fe/SiO_2/p-Si <B, Mn> interface and the role of the iron film is reduced only to the formation of bending zones in this region [18].

The observation of the linear dependence of the LPV on the position of the light spot in the studied structures can be understood if we assume that the metal film on the surface of the MOS structure serves only to create a surface bending of the zones into the silicon region adjacent to the SiO_2/Si interface, and the process of LPV generation occurs in the near-surface region of silicon. Depending on the degree of curvature of the zones in the near-surface region of silicon, inversion layers, depletion or enrichment are formed, and the resulting transitions of the type p-n, p^-p (n^-n) or p^+-p (n^+-n) are responsible for the observed effects. At the same time, the excess concentrations of photogenerated carriers will be greater than the main ones in both the p-region and the n-region [2].

Usually, the LPV generated was measured at the contacts located on the side opposite to the illumination. However, it has recently been shown that the sensitivity of LPE in MS and MOS structures can be increased by lighting and placing contacts from the side of the metal film. For example, in Ti/Si and Co/Si structures, the sensitivity of the LPE measured from the metal side is 1.45 times higher than the similar characteristic measured from the silicon side [7, 8, 11, 12]. Based on theoretical calculations, it can be concluded that the use of metals with high output performance and high resistivity in MOS structures leads to an increase in LPE.

The study of the effect of the contact distance on the value of the LPV showed that with an increase in the distance between the contacts, starting from a certain distance from both contacts, the value of the LPV becomes zero (Figure 7). As the contacts approach each other, the area on which the LPV is zero decreases, and at a certain value of the contact distance, this area disappears altogether.

This phenomenon seems to be related to generation-recombination processes in a semiconductor substrate. When the distances between the contacts are greater than the diffusive length of the non-basic charge carriers, i.e., $d > L_p, L_n$, the charge carriers formed under the action of light recombine without reaching the zone of action of the contact fields. When d becomes comparable to L_p, L_n, i.e., when the conditions $d \sim L_p, L_n$ are met, most of the generated charge carriers reach the contact field area and thus contribute to the LPE. This fact shows that based on the study of the LPV value, depending on the contact distances, it is possible to determine the numerical values of the diffusion lengths of minor current carriers (L_p and L_n), their lifetimes (τ_p and τ_n) and diffusion coefficients (D_p and D_n) on the substrate material.

To study the influence of the frequency of the radiation source on the magnitude and nature of the LPE, the dependences of the LPV of the studied structures on the frequency of radiation were removed (Figure 8). In our experiments, two diode-pumped semiconductor lasers with wavelengths of 532 and 632 nm and a power of 20 mW were used.

LPE has high sensitivity and linearity. The dependence of the LPE on the wavelength of laser radiation is shown in Fig. 8. As can be seen from Fig. 8, with an almost identical character, the change in the magnitude of the LFV and their magnitude depends on the wavelength. In addition, there is a significant asymmetry in the shape of the dependence of the

LPV on the contact distance. The value of the maximum LPV on the side of the negative electrode is significantly less than on the side of the positive electrode. For a red laser, these values are 300 and 210 MV, respectively. The value of the maximum LPV in the positive electrode for the red laser is almost 1.4 times greater than that of the green laser, at the same time, the value of this for the negative electrode is 1.2 times. This allows us to assume that for the study of LPE in Fe/SiO2/p-Si<B, Mn> HS, the most suitable laser wavelength is 632 nm, and LPE will increase with increasing laser radiation power in a certain range of power values and saturation is observed starting from a certain power value (Fig. 9). These results are in good agreement with the results of the study of LPE in Ni-SiO2-Si structures, where a laser with a wavelength of 632 nm is also suitable laser radiation for LPE [22].

The asymmetry of the shape of the LPV dependence on the contact distance is associated with an uneven distribution of charged impurity centers associated with manganese atoms. Since manganese in silicon is in a positively charged state, it is shifted towards the negative electrode under the action of the contact field, which leads to a decrease in the potential of the negative electrode. Figure 8 shows that the LPV value increases non-linearly with increasing laser power.

In the initial phase of the dependence, with laser power in the range of 0-6 mW, the LPV grows quasi-linearly, in the power range of 7-10 mW, the LPV grows very quickly and, starting from 11 mW, its growth slows down and reaches saturation, starting from 12 mW. In a certain wavelength range of laser radiation and at high power, repeated excitation of electron-hole pairs is possible. When the saturation state is reached, the LPV value does not change with increasing laser power. The LPV value at saturation depends on the laser frequency. Apparently, this is due to the possibility of multiple excitations of electron-hole pairs for different photons. Although the number of photogenerated electron-hole pairs increases with increasing laser power, the number of electrons that can be transferred by the built-in internal electric field is limited. The LPV value reaches saturation when the rate of generation of electron-hole pairs is equal to the rate of their recombination. Consequently, the LPV cannot increase indefinitely with increasing laser power. This is indirect evidence that the LPV is mainly due to electron diffusion, and not temperature effects.

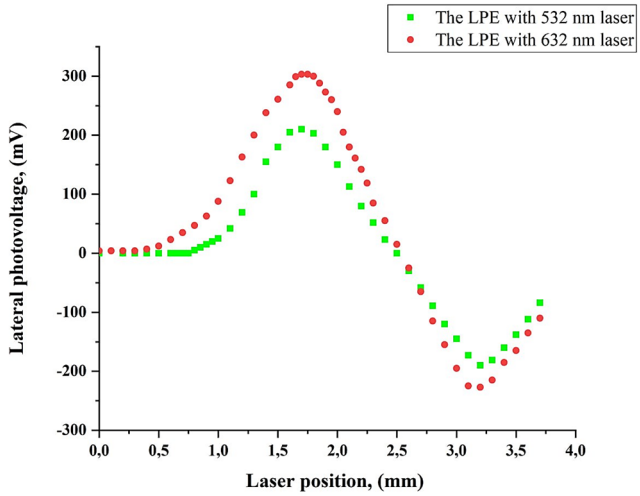

Figure 8. The dependence of the LPV on the wavelength of laser radiation with a power of 8 mW in HS Fe/SiO_2/p-Si<B, Mn>. The electrical resistivity of the sample ρ = 1×10^2 Ω×cm, T = 293 K

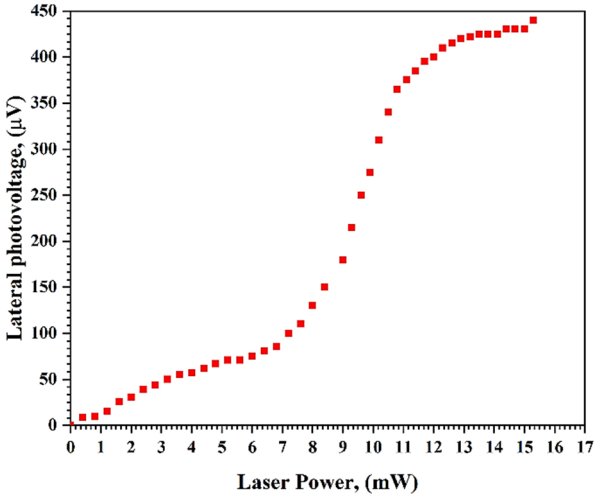

Figure 9. The dependence of the LPV on the laser power in the Fe/SiO_2/n-Si<B, Mn> HS. The electrical resistivity of the samples ρ = 1×10^5 Ω×cm, T = 293 K

The dependence of the LPV on the power of laser radiation, shown in Fig. 9, can be interpreted as follows. At low laser powers, the number of photogenerated pairs is small and their number increases linearly with increasing laser power, which corresponds to the linear growth of the LPV. Starting from a certain value of the laser radiation power, the number of generated carrier pairs increases non-linearly. This is due to the fact that at high laser radiation powers, it is possible to re-excite electron-hole pairs, which undoubtedly leads to a rapid increase in LPV. When the saturation state is reached, the LPV value does not change with increasing laser power. The LPV value at saturation depends on the laser frequency. Apparently, this is due to the possibility of multiple excitations of electron-hole pairs for different photons. Although the number of photogenerated electron-hole pairs increases with increasing laser power, the number of electrons that can be transferred by the built-in internal electric field is limited. The LPV value reaches saturation when the rate of generation of electron-hole pairs is equal to the rate of their recombination. Consequently, the LPV cannot increase indefinitely with increasing laser power. This is indirect evidence that LPV is mainly caused by electron diffusion, and not by temperature effects [18].

CONCLUSIONS

In this paper, the technology of obtaining HS of the Fe/SiO_2/p-Si<B, Mn> and Fe/SiO_2/n-Si<B, Mn> types and LPE in them is investigated.

Based on the results obtained, it can be concluded that the technology described by us allows obtaining fairly good HS. Experiments on the study of LPE have shown that a pronounced manifestation of LPV is observed in the studied HS.

In these HS, LPE is observed and the nature of the change in LPV depends on the contact distance, wavelength and power of the laser radiation.

Based on the LPV study, depending on the contact distance, it can be said that it is possible to determine the numerical values of the diffusion lengths of minor current carriers (L_p and L_n), their lifetimes (τ_p and τ_n) and diffusion coefficients (D_p and D_n) on the substrate material.

The nature of the change and the magnitude of the LPV depend on the concentration of charge carriers and the type of conductivity C, HC and OC of silicon samples. The observed features in HS are explained by the fact that in C, HC and OC silicon samples, impurities that create deep levels in the silicon band gap form various multicharged complexes that modulate the energy band of silicon, which underlies the observed effects in C, HC and OC silicon samples and HS based on them.

Author Contributions: Conceptualization, A.E.U. and S.F.A.; methodology, A.E.U. and S.F.A.; software, N.A.D. and A.U.A.; validation, S.T.S. and U.R.M.; formal analysis, S.T.S. and U.R.M.; R.; writing - review and editing, A.E.U., N.A.D.; writing – original draft preparation, A.E.U.

Funding: This research received no external funding.

Data Availability Statement: The data may partially be available through direct contact with the relevant authors.

Conflicts of Interest: The authors declare no conflict of interest.

ORCID

Eshkuvat U. Arzikulov, https://orcid.org/0000-0001-9179-3402; **Alisher D. Nurimov,** https://orcid.org/0009-0008-1291-3380

REFERENCES

[1] J. Henry, and J. Livingstone, "Improved position-sensitive detectors using high resistivity substrates," J. Phys. D: Appl. Phys. **41**, 165106 (2008). https://doi.org/10.1088/0022-3727/41/16/165106

[2] S.Q. Xiao, H. Wang, Z.C. Zhao, Y.Z. Gu, Y.X. Xia, and Z.H. Wang, "The Co-film-thickness dependent lateral photoeffect in Co-SiO_2-Si metal-oxide-semiconductor structures," Opt. Express. **16**, 3798-3806 (2008). https://doi.org/10.1364/OE.16.003798

[3] C.Q. Yu, H. Wang, S.Q. Xiao, and Y.X. Xia, "Direct observation of lateral photovoltaic effect in nano-metal films," Opt. Express, **17**, 21712-21722 (2009). https://doi.org/10.1364/OE.17.021712

[4] S. Wang, W. Wang, L. Zou, X. Zhang, J. Cai, Z. Sun, B. Shen, and J. Sun, "Magnetic Tuning of the Photovoltaic Effect in Silicon-Based Schottky Junctions," Adv. Mater. **26**(47), 8059–8064 (2014). https://doi.org/10.1002/adma.201403868

[5] S.H. Wang, X. Zhang, L.K. Zou, J. Zhao, W.X. Wang, and J.R. Sun, "Lateral resistance reduction induced by the light-controlled leak current in silicon-based Schottky junction," Chin. Phys. B, **24**(10), 107307 (2015). https://doi.org/10.1088/1674-1056/24/10/107307

[6] S.Q. Xiao, H. Wang, C.Q. Yu, Y.X. Xia, J.J. Lu, Q.Y. Jin, and Z.H. Wang, "A novel position-sensitive detector based on metal-oxide-semiconductor structures of Co–SiO_2–Si," New Journal of Physics, **10**(3), 033018 (2008). https://doi.org/10.1088/1367-2630/10/3/033018

[7] C. Yu, and H. Wang, "Large Lateral Photovoltaic Effect in Metal-(Oxide-) Semiconductor Structures," Sensors, **10**, 10155-10180 (2010). https://doi.org/10.3390/s101110155

[8] L. Chi, P. Zhu, H. Wang, X. Huang, and X. Li, "A high-sensitivity position-sensitive detector based on Au–SiO_2–Si structure," J. Opt. **13**(1), 015601 (2010). https://doi.org/10.1088/2040-8978/13/1/015601

[9] J.P. Cascales, I. Martínez, D. Díaz, J.A. Rodrigo, and F.G. Aliev, "Transient lateral photovoltaic effect in patterned metal-oxide-semiconductor films," Applied Physics Letters, **104**(23), 231118 (2014). https://doi.org/10.1063/1.4882701

[10] S. Liu, X. Xie, and H. Wang, "Lateral photovoltaic effect and electron transport observed in Cr nano-film," Opt. Express, **22**, 11627–11632 (2014). https://doi.org/10.1364/OE.22.011627

[11] I.A. Bondarev, M.V. Raustkii, and A.S.Tarasov, "Lateral photovoltaic effect in silicon-based hybrid structures under external magnetic field," Materials Science in Semiconductor Processing, **167**, 107786-107795 (2023). https://doi.org/10.1016/j.mssp.2023.107786

[12] X. Wang, B. Song, M. Huo, Y. Song, Z. Lv, Y. Zhang, Y. Wang, et al., "Fast and sensitive lateral photovoltaic effects in Fe_3O_4/Si Schottky junction," RSC Advances, **5**(80), 65048–65051 (2015). https://doi.org/10.1039/c5ra11872gX

[13] X. Huang, C. Mei, J. Hu, D. Zheng, Z. Gan, P. Zhou, and H. Wang, "Potential Superiority of p-Type Silicon-Based Metal–Oxide–Semiconductor Structures Over *n*-Type for Lateral Photovoltaic Effects," IEEE Electron Device Letters, **37**(8), 1018–1021 (2016). https://doi.org/10.1109/led.2016.2577700

[14] T.A. Pisarenko, V.V. Korobtsov, A.A. Dimitriev, V.V. Balashev, V.V. Zheleznov, and A.A. Yakovlev, "Giant lateral photovoltaic effect in the TiO_2/SiO_2/p-Si heterostructure," St. Petersburg Polytechnic University Journal. Physics and Mathematics, **15**, 32-37 (2022).

[15] M.C. Özdemir, Ö. Sevgili, I. Orak, and A. Turut, "Determining the potential barrier presented by the interfacial layer from the temperature induced I-V characteristics in Al/p-Si Structure with native oxide layer," Mater. Sci. Semicond. Process, **125**, 105629 (2021). https://doi.org/10.1016/j.mssp.2020.105629

[16] A. Ashery, M.M. Elnasharty, I.M. El Radaf, "Current Transport and Dielectric Analysis of Ni/SiO_2/p-Si Diode Prepared by Liquid Phase Epitaxy," Silicon, **14**, 153–163 (2022). https://doi.org/10.1007/s12633-020-00808-4

[17] A. Ashery, M.M. Elnasharty, A.A. Khalil, and A.A. Azab, "Negative resistance, capacitance in Mn/SiO_2/p-Si MOS structure," Mater. Res. Express, **7**, 085901 (2020). https://doi.org/10.1088/2053-1591/aba818

[18] X. Ling, P.F. Zhu, K. Song, and X. Li, "The lateral photovoltaic effect in the Ni-SiO_2-Si structure with bias," Research Square, 1-19 (2023). https://doi.org/10.21203/rs.3.rs-2903257/v1

[19] N.N.K. Reddy, S. Godavarthi, K.M. Kumar, V.K. Kummara, S.V.P. Vattikuti, H.Sh. Akkera, Y. Bitla, et al., "Evaluation of temperature dependent electrical transport parameters in Fe_3O_4/SiO_2/n Si metal–insulator semiconductor (MIS) type Schottky

barrier heterojunction in a wide temperature range," J. Mater. Sci. Mater. Electron. **30**, 8955–8966 (2019). https://doi.org/10.1007/s10854-019-01223-1
[20] N.V. Volkov, M.V. Rautskii, A.S. Tarasov, I.A. Yakovlev, I.A. Bondarev, A.V. Lukyanenko, S.N. Varnakov, and S.G. Ovchinnikov, "Magnetic field-driven lateral photovoltaic effect in the Fe/SiO_2/p-Si hybrid structure with the Schottky barrier,"' Physica E Low Dimens. Syst. Nanostruct. **101**, 201–207 (2018). https://doi.org/10.1016/j.physe.2018.03.027
[21] M.K. Bakhadirkhanov, N.F. Zikrillaev, S.B. Isamov, and S.V. Koveshnkov, in: *Photoelectrical Phenomenon in Silicon with multicharged nanoclusters*, (Technical University press, Tashkent, Uzbekistan, 2017). pp. 252-254.
[22] E.U. Arzikulov, and I.P. Parmankulov, "Vibrations of Photocurrent Induced by IR Light in Silicon with Quantum Dots," Surf. Eng. Appl. Electrochem. **44**, 504–507 (2008). https://doi.org/10.3103/S1068375508060148
[23] M.K. Bakhadyrkhanov, K.S. Ayupov, G.Kh. Mavlyanov, and S.B. Isamov, "Negative Magnetoresistance in Silicon with Manganese Atom Complexes $[Mn^+]^4$," Semicond. **44**, 1145–1148 (2010). https://doi.org/10.1134/S106378261009006X
[24] E.U. Arzikulov, and J.T. Ruzimurodov, "Magnetic Resistance of Silicon Specimens with Manganese Impurities," J. Commun. Technol. Electron. **52**, 1049–1053 (2007). https://doi.org/10.1134/S1064226907090148
[25] M.K. Bachadyrkhanov, S.B. Isamov, N.F. Zikrillaev, and E.U. Arzikulov, "Infrared Quenching of Photoconduction in Silicon with Multicharge Manganese Clusters," Surf. Eng. Appl. Electrochem. **49**, 308–311 (2013). https://doi.org/10.3103/S1068375513040029
[26] M.K. Bakhadyrkhanov, G.K. Mavlonov, S.B. Isamov, Kh.M. Iliev, K.S. Ayupov, Z.M. Saparniyazova, and S.A. Tacilin, "Transport properties of silicon doped with manganese via low-temperature diffusion," Inorg. Mater. **47**, 479–483 (2011). https://doi.org/10.1134/S0020168511050062
[27] M. Mebarki, A. Layadi, A. Guittoum, A. Benabbas, B. Ghebouli, M. Saad, and N. Menni, "Structural and electrical properties of evaporated Fe thin films," Appl. Surf. Sci. **257**(16), 7025–7029 (2011). https://doi.org/10.1016/j.apsusc.2011.02.114
[28] Y. Lin, J. Xie, H. Wang, Y. Li, C. Chavez, S. Lee, S.R. Foltyn, et al., "Green luminescent zinc oxide films prepared by polymer-assisted deposition with rapid thermal process," Thin Solid Films. **492**(1-2), 101–104 (2005). https://doi.org/10.1016/j.tsf.2005.06.060
[29] Z.B. Fang, Z.J. Yan, Y.S. Tan, X.Q. Liu, and Y.Y. Wang, "Influence of post-annealing treatment on the structure properties of ZnO films," Appl. Surf. Sci. **241**(3-4), 303–308 (2005). https://doi.org/10.1016/j.apsusc.2004.07.056

ЛАТЕРАЛЬНИЙ ФОТОЕЛЕКТРИЧНИЙ ЕФЕКТ У КРЕМНІЄВИХ ГІБРИДНИХ СТРУКТУРАХ ЗАЛІЗО-ДІОКСИД КРЕМНІЮ

Ешкуват У. Арзікулов[a], Алішер Д. Нурімов[a], Ф.А. Салахітдінов[a], У.А. Аширов[a], Т.С. Шарафова[a], А.С. Худжанов[b], Р.М. Усанов[a]

[a] *Самаркандський державний університет імені Шарофа Рашидова, м. Самарканд, Університетський бульвар 15, 140000, Республіка Узбекистан*

[b] *Самаркандський державний університет ветеринарної медицини, тваринництва і біотехнологій, м. Самарканд, вул. Мірзо Улуг Бек 77, 140003, Республіка Узбекистан*

У статті наведено експериментальні результати з технології отримання та дослідження латерального фотоефекту (ЛФЕ) в гібридних структурах типу (ГС) Fe/SiO_2/p-Si<B, Mn> та Fe/SiO_2/n-Si<B, Mn>. Технологія отримання таких ГС складається з двох частин: по-перше, отримання компенсованих (К), висококомпенсованих (ВК) і надкомпенсованих (НК) зразків Si<B, Mn>. По-друге, отримання HS Fe/SiO_2/p-Si<B, Mn> і Fe/SiO_2/n-Si<B, Mn>. На основі результатів показано, що було отримано достатньо хороший ГС. Експерименти по вивченню ЛФЕ показали, що в досліджуваних ГС спостерігається виражений прояв латерального фотоефекту, величина і характер якого сильно залежать від типу провідності та питомого опору компенсованого кремнію. Спостережувані особливості пояснюються тим, що в зразках кремнію К, ВК та НК домішки, які створюють глибокі рівні в забороненій зоні кремнію, утворюють різноманітні багатозарядні комплекси, які модулюють енергетичну зону кремнію, що призводить до суттєвих змін його фізико-хімічних та генераційно-рекомбінаційних властивостей, що лежить в основі спостережуваних ефектів. На основі досліджень ЛФЕ залежно від контактної відстані можна визначити чисельні значення дифузійних довжин другорядних носіїв струму (L_p та L_n), їх час життя (τ_p та τ_n) та коефіцієнтів дифузії (D_p та D_n) на матеріалі підкладки.

Ключові слова: *латеральний фотоефект; гібридна структура; компенсований кремній; фотонапруга; дифузія; випаровування; оксид; p-n перехід*